

REPORT DOCUMENTATION PAGE			Form Approved OMB No. 0704-0188	
Public reporting burden for this collection of information is estimated to average 1 hour per response, including the time for reviewing instructions, searching existing data sources, gathering and maintaining the data needed, and completing and reviewing the collection of information. Send comments regarding this burden estimate or any other aspect of this collection of information, including suggestions for reducing this burden to Washington Headquarters Services, Directorate for Information Operations and Reports, 1215 Jefferson Davis Highway, Suite 1204, Arlington, VA 22202-4302, and to the Office of Management and Budget, Paperwork Reduction Project (0704-0188), Washington, DC 20503.				
1. AGENCY USE ONLY (Leave blank)	2. REPORT DATE November 16, 1998	3. REPORT TYPE AND DATES COVERED Technical Report # 40		
4. TITLE AND SUBTITLE Solubilization and Encapsulation of Fullerenes by Amphiphilic Block Copolymers		5. FUNDING NUMBERS N00014-94-1-0540 Kenneth J. Wynne R & T Code 3132111		
6. AUTHOR(S) X. Linda Chen and Samson A. Jenekhe				
7. PERFORMING ORGANIZATION NAMES(S) AND ADDRESS(ES) University of Rochester Department of Chemical Engineering 206 Gavett hall, Box 270166 Rochester, NY 14627-0166		8. PERFORMING ORGANIZATION REPORT NUMBER # 40		
9. SPONSORING / MONITORING AGENCY NAMES(S) AND ADDRESS(ES) Office of Naval Research 800 North Quincy Street Arlington, VA 22217-5000		10. SPONSORING / MONITORING AGENCY REPORT NUMBER		
11. SUPPLEMENTARY NOTES Submitted to Langmuir		19981120 162		
a. DISTRIBUTION / AVAILABILITY STATEMENT Reproduction in whole or in part is permitted for any purpose of the United States Government. This document has been approved for public release and sale; its distribution is unlimited.		12. DISTRIBUTION CODE		
13. ABSTRACT (Maximum 200 words) Solubilization and encapsulation of fullerenes C <sub>60</sub> and C <sub>70</sub> by ultralarge hollow micelles formed by rod-coil diblock copolymers and characterization of the resulting self-organized fullerene-block copolymer assemblies are reported. The solubilization capacity of each fullerene in poly(phenylquinoline)-block-polystyrene (PPQ-PS) micelles in binary solvents, trifluoroacetic acid/dichloromethane and trifluoroacetic acid/toluene, was determined to be 200 mg fullerene per gram of PPQ-PS and found to be independent of block copolymer composition and concentration. This represents fullerene solubility enhancement by factors of 1040 and 63 compared to the solubilities in pure dichloromethane and toluene, respectively. Fullerenes C <sub>60</sub> and C <sub>70</sub> were found to change the micellization and self-assembly of PPQ-PS block copolymers in solution from polymorphic aggregates to only hollow spheres with encapsulated fullerenes. The solubilization and encapsulation of up to 1 - 10 billion fullerene molecules in PPQ-PS block copolymer micelles increased the aggregation number to over 10 <sup>9</sup> while the aggregate diameter increased from 1-5 µm to over 30 µm. Photoluminescence emission and excitation spectra of the fullerene-PPQ-PS block copolymer assemblies evidenced fullerene-induced J-aggregation of the conjugated PPQ blocks. In addition to providing the first detailed knowledge of the effects of solubilizates on the molecular packing of block copolymer micelles, the self-organized fullerene-block copolymer assemblies constitute novel mesoscopic supramolecular materials for electronic, optoelectronic, photonic and other applications. The present results also provide evidence of micellization and micellar solubilization phenomena at the 1 to 30 micrometer size scale.				
14. SUBJECT TERMS Amphiphilic block copolymers; solubilization of fullerenes; encapsulation of fullerenes; C <sub>60</sub> ; C <sub>70</sub> ; micelles; J-aggregation.		15. NUMBER OF PAGES 41		
		16. PRICE CODE		
17. SECURITY CLASSIFICATION OF REPORT Unclassified	18. SECURITY CLASSIFICATION OF THIS PAGE Unclassified	19. SECURITY CLASSIFICATION OF ABSTRACT Unclassified	20. LIMITATION OF ABSTRACT Unlimited	

OFFICE OF NAVAL RESEARCH

GRANT NO: N00014-94-1-0540

R&T Code 3132111

Kenneth J. Wynne

Technical Report NO. 40

Solubilization and Encapsulation of Fullerenes  
by Amphiphilic Block Copolymers

By

X. Linda Chen and Samson A. Jenekhe

Prepared for Publication

In

Langmuir

Department of Chemical Engineering  
University of Rochester, New York 14627

November 16, 1998

Reproduction in whole or in part is permitted for any purpose  
of the United States Government

This document has been approved for public release and sale;  
its distribution is unlimited.

X. Linda Chen and Samson A. Jenekhe\*

Departments of Chemical Engineering and Chemistry

University of Rochester, Rochester, New York 14627-0166

### Abstract

Solubilization and encapsulation of fullerenes  $C_{60}$  and  $C_{70}$  by ultralarge hollow micelles formed by rod-coil diblock copolymers and characterization of the resulting self-organized fullerene-block copolymer assemblies are reported. The solubilization capacity of each fullerene in poly(phenylquinoline)-*block*-polystyrene (PPQ-PS) micelles in binary solvents, trifluoroacetic acid/dichloromethane and trifluoroacetic acid/toluene, was determined to be 200 mg fullerene per gram of PPQ-PS and found to be independent of block copolymer composition and concentration. This represents fullerene solubility enhancement by factors of 1040 and 63 compared to the solubilities in pure dichloromethane and toluene, respectively. Fullerenes  $C_{60}$  and  $C_{70}$  were found to change the micellization and self-assembly of PPQ-PS block copolymers in solution from polymorphic aggregates to only hollow spheres with encapsulated fullerenes. The solubilization and encapsulation of up to 1 – 10 billion fullerene molecules in PPQ-PS block copolymer micelles increased the aggregation number to over  $10^9$  while the aggregate diameter increased from 1-5  $\mu\text{m}$  to over 30  $\mu\text{m}$ . Photoluminescence emission and excitation spectra of the fullerene-PPQ-PS block copolymer assemblies evidenced fullerene-induced J-aggregation of the conjugated PPQ blocks. In addition to providing the first detailed knowledge of the effects of solubilizates on the molecular packing of block copolymer micelles, the self-organized fullerene-block copolymer assemblies constitute novel mesoscopic supramolecular materials for electronic, optoelectronic, photonic and other applications. The present results also provide evidence of micellization and micellar solubilization phenomena at the 1 to 30 micrometer size scale.

## Introduction

The self-assembly of amphiphilic block copolymers in solution is currently of wide scientific and technological interests.<sup>1-21</sup> In a block selective solvent, amphiphilic block copolymers usually self-assemble into spherical micelles which consist of a core of the insoluble block and a shell of the solvated block.<sup>1-20</sup> Most block copolymer micelles typically have average diameters in the 20 to 80 nm range and aggregation numbers of the order 20 to 200.<sup>2,3,5,6,17</sup> One of the key properties of such micellar aggregates is that they can solubilize otherwise insoluble small molecules<sup>7-18</sup> and homopolymers.<sup>19</sup> Many of the actual or potential applications of block copolymer micelles arise from this capability to enhance the solubility of substances or solubilization phenomena. Examples include delivery vehicles for drugs and agricultural chemicals, scavengers for pollutants, mesoscale environment for materials synthesis, micellar catalysis, and chemical extraction aids in separation processes.<sup>1-5</sup>

Extensive theoretical<sup>1, 7-11</sup> and experimental<sup>1-3, 12-20</sup> studies of solubilization phenomena in block copolymer micelles have been reported. Some of the pertinent findings include the following. The presence of the solubilized substance (solubilizate) can greatly enhance the micellization process as shown by a decrease of the critical micelle concentration (cmc) and an increase in the aggregation number ( $g_n$ ).<sup>7-11,17</sup> Block copolymer architecture (AB diblock, ABA and BAB triblocks), composition, molecular weight, and block lengths ( $N_A$ ,  $N_B$ ) can significantly influence the solubilization capacity,  $g_n$ , and cmc.<sup>8,11,19b</sup> Solubilization can induce major changes in the size and shape of block copolymer micelles.<sup>7-20</sup> The increase in micellar core diameter, and hence the overall size of the micellar aggregate, arises from both the incorporation of the solubilizate into the core and the increase in the number of block copolymer chains ( $g_n$ ) accommodated in the micelle.<sup>8,11,14,17</sup> Many solubilizates have been investigated in

aqueous and nonaqueous media, including aromatic molecules such as benzene, toluene, naphthalene, pyrene and anthracene.<sup>1,2,12,15-16,18,20</sup> Strong solubilize-core block interactions are predicted to play a major role in the solubilization behavior of block copolymer micelles.<sup>7-9,11</sup>

Studies of self-assembly of block copolymers in solution and related solubilization phenomena have been largely focused on coil-coil block copolymer architectures.<sup>1-20</sup> We recently reported the self-assembly of unusually large, geometrically well-defined, and polymorphic aggregates from solutions of novel rod-coil diblock copolymers, poly(phenylquinoline)-*block*-polystyrene (PPQ-PS).<sup>21</sup> Hollow spheres, tubules, lamellae and doughnuts with sizes in the 1-50  $\mu\text{m}$  range and aggregation numbers of up to  $10^8$  were observed, making the rod-coil block copolymer assemblies comparable in size to bacteria and mammalian cells.<sup>21</sup> In particular, the spherical PPQ-PS aggregates had some features characteristic of micelles: for example, an aggregate structure consisting of a monolayer rather than a bilayer. However, unlike conventional micelles the spherical aggregates have a large hollow cavity akin to vesicles. The spherical PPQ-PS assemblies have a novel micellar aggregate structure: a hollow cavity core, an inner PS shell and an outer PPQ shell.<sup>21</sup> The unusual self-assembling mesostructures of these rod-coil block copolymers in solution suggest that they may have novel solubilization properties and allow solubilization phenomena to be probed at new size scales and by new approaches.

In this paper, we report a study of solubilization phenomena in amphiphilic rod-coil diblock copolymer solutions. We show that PPQ-PS diblock copolymers exhibit micelle-like, high capacity, solubilization and encapsulation of fullerenes  $\text{C}_{60}$  and  $\text{C}_{70}$ . Optical absorption spectroscopy and a combination of optical microscopy with mass balance have been used to determine the solubilization capacity of fullerenes in PPQ-PS block copolymers and their

aggregation numbers. Direct microscopic evidence of fullerene solubilization induced changes in the size, aggregation number, and shape of the block copolymer aggregates is presented. Photoluminescence emission (PL) and excitation (PLE) spectroscopies were also used to probe the effect of fullerene solubilization and encapsulation on aggregate molecular packing.

Fullerenes and carbon nanotubes are currently of interest in many areas of science and technology.<sup>22-28</sup> For example, pure alkali metal (Li, Na, K, Rb, Cs) complexes of C<sub>60</sub> are being investigated because of their relatively high superconducting transition temperatures of up to 30-40 K.<sup>22, 25</sup> Superconductivity has also been discovered in fullerene/conducting polymer composites.<sup>26</sup> Composites of fullerenes with various conjugated polymers or photoconductive polymers are known to undergo efficient photoinduced electron transfer, leading to very good photoconductors of interest for imaging, photodetectors, and photovoltaic cells.<sup>27, 28</sup> However, the poor solubility of fullerenes in organic solvents has been a major challenge to the large scale extraction, purification, processing and application of the pure nanostructured carbon materials and their blends with polymers.<sup>22-23, 29-30</sup> Fullerenes C<sub>60</sub> and C<sub>70</sub> with outer diameters of about 1.0 and 1.15 nm,<sup>22, 23</sup> respectively, are large molecules whose sizes are in the lower limit of colloidal particles.<sup>31</sup> In addition to learning how to enhance the solubility and processability of such large molecules, our solubilization and encapsulation studies of fullerenes in amphiphilic block copolymers also aim to develop methods for the self-assembly of functional fullerene/block copolymer mesostructures.

The chemical structure of the rod-coil diblock copolymers, PPQ-PS, used in our solubilization and encapsulation studies is shown in scheme 1. The synthesis, characterization, and detailed morphological studies of the pure diblock copolymers will be described elsewhere.<sup>32</sup> A preliminary report on the same diblock copolymers has appeared.<sup>21</sup> The parent rodlike

homopolymer, poly(phenylquinoline) (PPQ), is an electroactive and photoactive conjugated polymer whose synthesis,<sup>33,34a</sup> optical,<sup>34</sup> electrochemical,<sup>34b</sup> optoelectronic and electroluminescent<sup>35</sup> properties have been reported. The intrinsic electroactive and photoactive properties of PPQ-PS diblock copolymers facilitated the use of absorption and emission spectroscopies and fluorescence microscopy in our studies.

## Experimental Section

**Materials.** The two copolymer compositions of poly(phenylquinoline)-*block*-polystyrene used in this study, denoted here as PPQ<sub>50</sub>PS<sub>300</sub> and PPQ<sub>10</sub>PS<sub>300</sub>, were synthesized by coupling functionalized polystyrene (PS) with the PPQ monomer, 5-acetyl-2-aminobenzophenone,<sup>33</sup> followed by polycondensation synthesis of the PPQ block. The starting monofunctionalized PS had a reported number average degree of polymerization of 300 and a polydispersity of 1.05 (Aldrich). The number average degree of polymerization of the PPQ blocks was determined from <sup>1</sup>H NMR spectra, thermal analysis, and other data.<sup>32</sup> A detailed description of the synthesis will appear elsewhere.<sup>32</sup>

Analytical grade solvents trifluoroacetic acid (TFA), dichloromethane (DCM), carbon disulfide (CS<sub>2</sub>), and toluene were purchased from Aldrich and used as received. Fullerene molecules C<sub>60</sub> (TCI, 99.9 %) and C<sub>70</sub> (Aldrich, 99 %) were used as received. Poly(ethylene oxide) (PEO) (M<sub>w</sub> of 5,000,000, M<sub>w</sub>/M<sub>n</sub> ~2.8), poly (methyl methacrylate) (M<sub>w</sub> of 350,000, M<sub>w</sub>/M<sub>n</sub> ~1.15) and polystyrene (M<sub>w</sub> of 6,000,000, M<sub>w</sub>/M<sub>n</sub> ~1.2) were purchased from Polysciences, Inc. (Warrington, PA) and used as received.

**Micellization and Solubilization Procedures.** Solutions of PPQ<sub>50</sub>PS<sub>300</sub> and PPQ<sub>10</sub>PS<sub>300</sub> were prepared by dissolving each copolymer in trifluoroacetic acid/dichloromethane (TFA/DCM) or TFA/toluene mixtures of various solvent volume ratios, 4/1, 2/1, 1/1, 1/4. The resulting

solutions had concentrations of 0.35 to 3.5 mg/ml (0.05 to 0.5 wt%) of diblock copolymers. The critical micelle concentration (cmc) of PPQ-PS block copolymers in these binary solvents is unknown but much less than order  $10^{-3}$  wt%. A known amount of fullerene ( $C_{60}$  or  $C_{70}$ ) was then added to each pre-made copolymer solution. Alternatively, fullerene/copolymer solutions were prepared by adding known amounts of solid polymer and fullerene to the binary TFA/DCM or TFA/toluene at the same time to achieve solutions with similar concentrations. We have also prepared fullerene/copolymer solutions by mixing a solution of fullerene in DCM or in toluene with a pre-made copolymer solution. Different weight fractions of fullerene to copolymer were employed, ranging from 0.01 to 50 wt. %. Preparation of solutions and the solubilization process took place at room temperature (25 °C) without heating or mechanical stirring. The fullerene/copolymer solutions were then stored for at least 2 days to equilibrate before assessment of solubilization and preparation of samples of the fullerene/block copolymer aggregates for microscopic observation and spectroscopic study.

Films (~1 to 20  $\mu\text{m}$  thick) resulting from drying the dilute solutions of block copolymer/solubilized fullerenes on glass slides at room temperature were investigated as made, or after treating them in 5 % triethylamine/ethanol (to remove any trace acids), and drying in a vacuum oven at 60°C for 24 hours. The films were investigated by polarized optical and fluorescence microscopies as well as by UV-Vis absorption and photoluminescence spectroscopies.

Preliminary experiments on the release of encapsulated fullerenes were done by placing dried fullerene/copolymer aggregates in either good solvents for the rigid-rod PPQ block (fresh, clear, 1:1 TFA:DCM or TFA:toluene solvent mixtures) or good solvents for the coil-like PS block (pure DCM or toluene). Release of encapsulated fullerene was monitored by optical absorption

spectroscopy to track any absorption signals of fullerene in solution.

**Optical Absorption Spectroscopy.** Absorption spectra of solutions (0.1 wt%) of fullerene  $C_{60}$  and  $C_{70}$  in  $CS_2$  were obtained using a quartz cuvet which was sealed by wax to prevent solvent evaporation. Absorption spectra of the pure  $PPQ_{50}PS_{300}$  and  $PPQ_{10}PS_{300}$  were similarly obtained in 1:1 TFA:DCM solutions at 0.1 wt% which is orders of magnitude larger than their cmc. These were used as the reference spectra for comparing the absorption spectra of solubilized fullerene/block copolymer micelles. The UV-Vis absorption spectra of all fullerene/PPQ-PS dispersions were obtained in 1-mm cuvet at room temperature (25 °C) and used to estimate the solubilization capacities of the fullerene/PPQ-PS systems. For this purpose the absorbance of each UV-Vis spectrum was normalized at a characteristic  $C_{60}$  or  $C_{70}$  absorption band. The normalized absorbance was then plotted as a function of the amount of fullerene added to a dispersion. The saturation of the normalized absorbance versus fullerene loading provided an estimate of the maximum amount that was solubilized.

The normalized absorbance  $X$  of solutions of  $C_{60}$ /diblock copolymers at 330 nm is given by  $X = C \cdot N_A \cdot [A_{330} - A_{330}^0] / [A_{422} - A_{422}^0]$ , where  $X$  is proportional to  $C_{60}$  solubilized per diblock copolymer chain in solution,  $C$  is a constant, which is the ratio of the absorption coefficients of PPQ block at 422 nm and  $C_{60}$  at 330 nm,  $N_A$  is the number of repeat units of PPQ in the diblock copolymer, and  $A_{330}$  and  $A_{422}$  are the absorbances at 330 and 422 nm, respectively.  $A_{330}^0$  is the calculated absorbance of PPQ at 330 nm whereas  $A_{422}^0$  is the calculated absorbance of  $C_{60}$  at 422 nm. Because of the negligible absorbance of  $C_{60}$  at 422 nm,  $A_{422}^0 = 0$ . For solutions of  $C_{70}$ /diblock copolymers, the normalized absorbance is  $Y = C \cdot N_A \cdot [A_{473} - A_{473}^0] / [A_{335} - A_{335}^0]$ , where  $Y$  is proportional to  $C_{70}$  solubilized per diblock copolymer chain,  $C$  is a constant, which is the ratio of the absorption coefficients of PPQ at 335 nm and  $C_{60}$  at 473 nm,  $N_A$  is the number of

repeat units of PPQ in the diblock copolymer, and  $A_{335}$  and  $A_{473}$  are the absorbances at 335 and 473 nm, respectively.  $A_{335}^0$  is the calculated absorbance of  $C_{60}$  at 335 nm whereas  $A_{473}^0$  is the calculated absorbance of PPQ at 473 nm. Because of the negligible absorbance of PPQ at 473 nm,  $A_{473}^0 = 0$ .

Films of solid aggregates were too scattering in the visible to obtain normal optical absorption spectra. Dilute solution optical absorption spectra of the pure fullerene and fullerene/copolymer samples, and those of thin films of block copolymers dispersed (0.1 wt%) in poly (ethylene oxide) (PEO) were recorded on a Perkin-Elmer Model Lambda 9 UV/VIS/NIR Spectrophotometer. All spectra were obtained at room temperature (25 °C).

**Optical and Fluorescence Microscopies.** Samples for observation by polarized optical microscopy (POM) and fluorescence microscopy (FM) were prepared by allowing several drops of a fullerene/block copolymer solution in TFA:DCM or TFA:toluene to spread and dry on glass slides. The various drying conditions explored were described above and were found not to influence the observed morphologies of aggregates (size, shape, and their distributions). Observations were made on an Olympus Model BX60 Fluorescence Optical Microscope and optical (bright field, polarized light) and fluorescence images were recorded by a digital camera.

**Photoluminescence Spectroscopy.** Photoluminescence (PL) and photoluminescence excitation (PLE) spectra were obtained on a Spex Fluorolog-2 spectrofluorimeter. Thin films of aggregates were measured by using the front face geometry in which samples were positioned such that the emission was detected at 22.5° from the incident radiation beam. Further details of the photophysical experimental techniques used here are similar to those we have described in detail elsewhere.<sup>36</sup>

**Differential scanning calorimetry (DSC).** The DSC thermograms were obtained on a Du Pont Model 2100 Thermal Analyst based on an IBM PS/2 Model 60 computer and equipped with a Model 910 DSC unit. The DSC thermograms of samples were obtained in nitrogen at a heating rate of 10 °C/min. Samples for DSC measurements were prepared by casting films of fullerene/PPQ<sub>50</sub>PS<sub>300</sub> solutions in TFA/DCM (1/1, v/v) onto glass slides and carefully removing vacuum dried fullerene-containing aggregates from glass slides into DSC sample pans by using a sharp razor blade. Before the aggregates were removed from the glass slides, they were observed by an optical microscope to ascertain their spherical micellar morphology. In the case of fullerene/polystyrene and fullerene/poly(methyl methacrylate) samples, drops of solutions in CS<sub>2</sub> were dried directly in aluminum DSC pans.

## Results and Discussion

**1. Micellar Solubilization of Fullerenes.** PPQ-PS solutions in the two binary solvent systems TFA/DCM and TFA/toluene were previously shown to undergo self-organization to produce hollow spheres, tubules and other aggregates.<sup>21</sup> Both solvent systems are selective for the PPQ block and are highly polar. Both C<sub>60</sub> and C<sub>70</sub> were insoluble in pure TFA or TFA/DCM or TFA/toluene mixtures (4/1 to 1/4, v/v) even though the fullerenes are slightly soluble in pure DCM (0.192 mg/g) and pure toluene (3.16 mg/g). We found that both C<sub>60</sub> and C<sub>70</sub> readily dissolved in these binary solvents at room temperature (25°C) when either PPQ<sub>50</sub>PS<sub>300</sub> or PPQ<sub>10</sub>PS<sub>300</sub> was present as illustrated in scheme 1. Optical absorption experiments on the resulting solutions showed strong characteristic fullerene absorption bands,<sup>22-23</sup> indicating the presence of fullerene in solution and hence evidence enhanced solubility facilitated by the amphiphilic block copolymers.

Figure 1 shows the absorption spectra of TFA/DCM solutions of pure PPQ<sub>50</sub>PS<sub>300</sub> (Fig. 1a), PPQ<sub>50</sub>PS<sub>300</sub> with 5 wt % C<sub>60</sub> (Fig 1b), together with the spectrum of pure C<sub>60</sub> in CS<sub>2</sub> (Fig. 1c). The spectrum of C<sub>60</sub>/PPQ<sub>50</sub>PS<sub>300</sub> blend solution showed absorption bands characteristic of the two components, C<sub>60</sub> and the diblock copolymer PPQ<sub>50</sub>PS<sub>300</sub>. The absorption band in the 370-460 nm region with maxima at 405 nm is due to the PPQ block of the copolymer. The sharp peak at 330 nm is due to the optical transition of C<sub>60</sub>. The magnified version of the blend spectrum in the 400-700 nm region is shown as the insert of Figure 1. The absorption bands with  $\lambda_{\text{max}}$  at 540 and 600 nm are characteristic absorption bands of C<sub>60</sub>. Figure 2 shows the absorption spectra of 5 wt % C<sub>70</sub>/PPQ<sub>50</sub>PS<sub>300</sub> and 5 wt % C<sub>70</sub>/PPQ<sub>10</sub>PS<sub>300</sub> in TFA/DCM and C<sub>70</sub> in CS<sub>2</sub>. The characteristic C<sub>70</sub> absorptions at 335, 383 and 473 nm and PPQ-PS absorption centered at 405 nm were observed in the C<sub>70</sub>/PPQ-PS solution spectra which could be readily deconvoluted into the component spectra. The fact that the absorption spectra of the C<sub>60</sub>/PPQ<sub>50</sub>PS<sub>300</sub> and C<sub>70</sub>/PPQ<sub>50</sub>PS<sub>300</sub> solutions are a superposition of the two chromophoric components (fullerene and pure diblock copolymer) suggests that there is no ground state electronic interaction between the fullerenes and the conjugated PPQ segments. This is to be expected since the fullerenes C<sub>60</sub> and C<sub>70</sub> are strong electron accepting molecules<sup>22-28</sup> as are the conjugated polyquinolines.<sup>33-35</sup> Therefore, absorption spectroscopy could be used to quantify the solubilization capacity of fullerenes in the block copolymer solutions.

All solubilization studies and solution optical absorption measurements were done on the four basic systems: C<sub>60</sub>/PPQ<sub>50</sub>PS<sub>300</sub>, C<sub>60</sub>/PPQ<sub>10</sub>PS<sub>300</sub>, C<sub>70</sub>/PPQ<sub>50</sub>PS<sub>300</sub>, and C<sub>70</sub>/PPQ<sub>10</sub>PS<sub>300</sub>. In addition to the two different approaches to preparing solubilized fullerene/block copolymer solutions illustrated in scheme 1, i.e., addition of solid fullerene to a pre-existing copolymer solution and addition of both fullerene and block copolymer to the solvent mixture, we also

prepared fullerene/PPQ-PS solutions by mixing a solution of fullerene in DCM with a pre-made copolymer solution. No discernible differences were observed between the three methods. Similar solution absorption spectra and, subsequently, similar aggregate morphologies were obtained. This suggested that the observed solubilization behavior is likely near equilibrium conditions.

Normalized absorbancies of the characteristic fullerene absorption bands were used as measures of the relative amounts of fullerene solubilized in the block copolymer solutions. Figure 3a shows plots of normalized  $C_{60}$  absorbance at 330 nm (see Experimental Section) versus  $C_{60}$  loading into the solution (mg  $C_{60}$  per g diblock copolymer in solution). The relative amount of solubilized  $C_{60}$  increased linearly with the fullerene loading of the diblock copolymer solutions, reaching saturation at a loading of about 200 mg/g. We take this limit as the solubilization capacity of the block copolymer solutions. It is noteworthy that the  $C_{60}$  solubilization characteristics of PPQ<sub>50</sub>PS<sub>300</sub> and PPQ<sub>10</sub>PS<sub>300</sub> are essentially identical as are the different copolymer concentrations (Fig. 3a). Similar data of normalized absorbance versus loading for  $C_{70}$  are shown in Figure 3b. A solubilization capacity of ~200 mg fullerene  $-C_{70}/g$  diblock copolymer is obtained. This is identical to the  $C_{60}$  result. The solubilization capacity of 200 mg/g translates to 11.8 and 9.2 solubilized  $C_{60}$  molecules per diblock chain for PPQ<sub>50</sub>PS<sub>30</sub> and PPQ<sub>10</sub>PS<sub>300</sub>, respectively. Similarly, the maximum amount of solubilized  $C_{70}$  molecule per diblock chain of PPQ<sub>50</sub>PS<sub>300</sub> and PPQ<sub>10</sub>PS<sub>300</sub> are 10.1 and 7.9, respectively.

The measured solubilization capacity of 200 mg of solubilized fullerene ( $C_{60}$  or  $C_{70}$ ) per gram of diblock copolymer represents a solubility enhancement by factors of 1040 and 63 compared to the solubilities in pure dichloromethane and toluene, respectively. The best previously reported, organic solvent for  $C_{60}$  is 1-chloronaphthalene which has a solubility limit

of 42.7 mg/g at room temperature (22°C).<sup>22,29,30</sup> The large enhancement of fullerene solubility in organic solvents by amphiphilic block copolymer micelles that is demonstrated here is thus very promising for potential applications in the large scale extraction, purification, and processing of fullerenes.<sup>22,23</sup>

In preliminary experiments on the release of encapsulated fullerenes, PPQ-PS micellar aggregates containing 1 and 5 wt % fullerenes C<sub>60</sub> and C<sub>70</sub> from TFA/DCM and TFA/toluene solutions were dried and then placed in pure DCM or toluene, which are good solvents for PS block, for several days. Release of any encapsulated fullerene was not observed by optical absorption spectroscopy which did not detect any absorption signals of fullerene in solution. Subsequent examination of these aggregates by optical microscopy showed that there was no change in the morphology, before and after their immersion in the *aprotic* organic solvents. However, when similarly dried aggregates were immersed in TFA/DCM or TFA/toluene solvent mixture (1/1, v/v), they dissolved and progressively released fullerene into solution as judged by absorption spectroscopy which revealed and could be used to track the fullerene absorption signal in solution. Although more detailed studies are necessary to quantify the release kinetics and behavior of encapsulated fullerenes in block copolymer assemblies, the preliminary indication is that the release could be triggered and controlled by pH.

Given the novel hollow structure and very large sizes of PPQ-PS micelles and some of the unusual features of their solubilization of fullerenes, it is not obvious that current theories of block copolymer micellization and solubilization can explain the experimental results.<sup>7-11</sup> One basic issue is whether the observed solubilization of fullerenes by PPQ-PS diblock copolymer assemblies is a *micellar solubilization phenomenon*<sup>1-20</sup> or *vesicle-like trapping*<sup>37</sup> or a hybrid of both. Arguing in favor of a micellar mechanism include: the similarity of the solubilization

capacity regardless of the self-assembly path (scheme1) which implies that the solubilized fullerene/PPQ-PS assemblies are thermodynamically very stable structures; as will be shown in the next two sections on aggregate morphology, fullerene solubilization causes major changes in the physical size, aggregation number, shape, and molecular packing of PPQ-PS aggregates. On the other hand, independence of solubilization capacity from copolymer concentration in solution and from the PPQ block length ( $N_A \sim 10$  and  $50$ ) is not a common feature of block copolymer micelle solubilization<sup>7-11</sup> but may reflect the hollow cavity of these assemblies. Nevertheless, some aspects of the results can be rationalized in terms of micellar solubilization theory for block copolymers.<sup>7-11</sup> From the known solubility parameters of fullerene- $C_{60}$  ( $\delta_f$ )<sup>22</sup> and polystyrene ( $\delta_{ps}$ )<sup>38</sup> which are 10 and 8.7 to 9.9 at 25°C, respectively, the Flory-Huggins interaction parameter  $\chi_{f,ps}$  expressed in terms of the solubility parameters<sup>7</sup>  $\chi_{f,ps} = (\delta_f - \delta_{ps})^2 v_f / k_B T$  is as small as 0.015, where  $v_f$  is molar volume,  $k_B$  is the Boltzmann's constant, and  $T = 298K$ . This suggests that there is strong interaction between fullerene and the PS blocks. Prior investigations of  $C_{60}$  solubility in many organic solvents have shown that the largest solubilities were observed in solvents with solubility parameters close to that of  $C_{60}$ .<sup>22,29,30</sup>

**2. Block Copolymer Aggregates with Encapsulated Fullerenes.** We have extensively investigated the morphology of fullerene-containing block copolymer aggregates which are dried from solutions. Unlike the multiple aggregate morphologies (hollow spheres, tubules, lamellae, and doughnuts) observed in the pure  $PPQ_{50}PS_{300}$  and  $PPQ_{10}PS_{300}$  diblock copolymers,<sup>21,32</sup> solid films from all fullerene-containing copolymer solutions with fullerene/copolymer ratios of 0.1 to 6 wt % showed only spherical aggregates. Films cast from solutions with fullerene concentration below this range were similar to the pure diblock copolymer solutions in exhibiting multiple aggregate morphologies. This means that the

solubilized fullerenes at this dilute loading are encapsulated in some of the aggregates without influencing the block copolymer self-organization process in solution. At fullerene loading of 7 wt % or higher, the solid films showed mixed morphologies consisting of spherical aggregates with encapsulated fullerene as well as needle-like crystals of the pure  $C_{60}$  or  $C_{70}$ .

Figures 4-6 show the typical morphologies of PPQ<sub>50</sub>PS<sub>300</sub> aggregates with encapsulated fullerenes revealed by optical and fluorescence microscopies. Figure 4 shows the fluorescence (4a, b) and polarized optical (4c) micrographs of a 0.1 wt %  $C_{70}$ /PPQ<sub>50</sub>PS<sub>300</sub> copolymer sample. Only spherical aggregates, with a typical diameter of about 10  $\mu$ m, were observed. The spherical aggregates have highly ordered structures as indicated by the polarized optical micrographs such as that shown in Figure 4c. Compared to the typical spherical aggregates of pure PPQ<sub>50</sub>PS<sub>300</sub> which were about 5  $\mu$ m in diameter, an enlargement of about a factor of 2 results from  $C_{70}$  encapsulation, even at this low loading level. Also, we note that these aggregates with encapsulated  $C_{70}$  are not very perfect spheres, having many rough surfaces and edges. In contrast, the empty hollow spheres from all the diblock copolymers had perfectly round geometry and very smooth surfaces when compared on the same size scale. Figure 4d shows a typical morphology of fullerene- $C_{60}$  encapsulated in PPQ<sub>50</sub>PS<sub>300</sub> at 0.1 wt % loading. The spherical aggregates were very similar in size, shape and size uniformity to the PPQ<sub>50</sub>PS<sub>300</sub> aggregates containing 0.1 wt %  $C_{70}$ .

Figures 5 and 6 show the photomicrographs of 1%  $C_{60}$ /PPQ<sub>50</sub>PS<sub>300</sub> and 6%  $C_{60}$ /PPQ<sub>50</sub>PS<sub>300</sub> samples, respectively. The average diameter of the aggregates in Figure 5 is 20  $\mu$ m. Fluorescence imaging showed the aggregates to be bright red in color (Fig. 5a, b). Under crossed polarizers, the same aggregates show yellow-brown color (Fig. 5c). At a loading of 6 wt %  $C_{60}$ , the average diameter of the highly spherical aggregates of Figure 6 is 30  $\mu$ m. These

aggregates were relatively uniform in size distribution and they have highly ordered structures with deep reddish-brown color under crossed polarizers.

Optical microscopy observation of films cast from solutions with high solubilized fullerene loading ( $\geq 7$  wt %  $C_{60}$  or  $C_{70}$  in PPQ<sub>50</sub>-PS<sub>300</sub>) showed the coexistence of the discrete spherical aggregates observed at smaller fullerene loading with needle-like and continuous fullerene phases. Optical micrographs of PPQ<sub>50</sub>PS<sub>300</sub> copolymer with 8 and 10 wt % solubilized  $C_{60}$  are shown in Figure 7. In addition to spherical aggregates with average diameters in the 10-20  $\mu\text{m}$  range, large needle-like phases (up to 10-20  $\mu\text{m}$  wide x 200  $\mu\text{m}$  long) characteristic of the pure  $C_{60}$  were also observed.

Figure 8 shows the average aggregate diameter, measured from the optical and fluorescence micrographs, as a function of fullerene loading in the four different fullerene/PPQ-PS systems. One main feature of the data is that at all fullerene loadings,  $C_{70}$ /PPQ<sub>50</sub>PS<sub>300</sub> aggregates have the largest sizes. However, there is no clear difference in size between the  $C_{70}$  – and  $C_{60}$  – containing aggregates of PPQ<sub>10</sub>PS<sub>300</sub>. These results suggest that there is both an effect of fullerene size on the fullerene/PPQ-PS aggregates size ( $C_{70} > C_{60}$ ) as well as a dependence on the rodlike block length (PPQ<sub>50</sub>PS<sub>300</sub> > PPQ<sub>10</sub>PS<sub>300</sub>). Another notable feature of the data is the trend of aggregate size with fullerene loading. Increase of diameter with encapsulated fullerene amount is observed to peak at about 60-70 mg/g which is followed by a factor of 2-3 decrease in size at fullerene loadings greater than 70 mg/g. The apparent 70-mg/g transition point may be regarded as the encapsulation capacity of the fullerenes in the block copolymer assemblies; that is, the maximum fullerene loading level where complete sequestering inside the spherical block copolymer aggregates is ensured as evidence by the morphological observations (Figure 4-7). Since this loading level (70 mg/g) is much smaller than the amount of fullerene that can be

solubilized (200 mg/g) as determined by solution absorption spectroscopy, this raises questions about the origin for this difference. One possibility is that the excess fullerene molecules outside the spherical aggregates (see for example Figure 7) were originally solubilized inside the nonspherical aggregates (tubules, lamellae, doughnuts) which were destabilized. Another possibility is that some of the fullerene molecules in solution exhibit colloidal interactions with the block copolymer molecules and micelles. Clearly, future experimental and theoretical studies to fully elucidate fullerene/block copolymer micelles is warranted.

We have estimated the aggregation number  $g_n$  of the self-organized fullerene/PPQ-PS assemblies from optical and fluorescence micrographs taken over large areas in conjunction with mass balance. For example, for the 6 wt %  $C_{60}$ /PPQ<sub>50</sub>PS<sub>300</sub> assembly,  $10^3$  spherical aggregates per mm<sup>2</sup> area was measured from a photomicrograph taken from a 0.2 mg sample covering a 5 cm<sup>2</sup> area. This information translates to  $9.6 \times 10^{-15}$  mole PPQ<sub>50</sub>PS<sub>300</sub> diblock/aggregate or  $g_n = 6 \times 10^9$ . Furthermore, the 6 wt %  $C_{60}$  or 64 mg/g encapsulated is equivalent to 3.7  $C_{60}$  molecules per PPQ<sub>50</sub>PS<sub>300</sub> diblock chain which in combination with  $g_n$  means that about  $2.2 \times 10^{10}$  fullerene- $C_{60}$  molecules are encapsulated inside each aggregate of Figure 6. Similar estimates of the number of  $C_{60}$  encapsulated in the PPQ<sub>50</sub>PS<sub>300</sub> spherical micelles at 0.1 and 3 wt % fullerene loading are  $4 \times 10^8$  and  $2 \times 10^9$ , respectively. Since a similar estimate of  $g_n$  for the empty PPQ<sub>50</sub>PS<sub>300</sub> is  $1.5 \times 10^8$ , these results suggest that fullerene solubilization and encapsulation enhances the aggregation number by factors of 2.7, 13, and 150 respectively at 0.1, 3, and 6 wt %  $C_{60}$  loading. Although such an enhancement of  $g_n$  is qualitatively consistent with the predictions of current theories for solubilization by micelles formed by coil-coil block copolymer,<sup>7-11</sup> it remains to establish their applicability to the unusually large micelles of PPQ-PS block copolymers. Compared to the typical  $g_n$  values of 50-100 for coil-coil block copolymer micelles,

<sup>1-20</sup> the aggregation number of the present PPQ-PS rod-coil block copolymer micelles is about 6 to 7 orders of magnitude larger.

To further shed light on the nature of PPQ-PS aggregates with encapsulated fullerenes, differential scanning calorimetry (DSC) was done on fullerene- $C_{60}$ /PPQ<sub>50</sub>PS<sub>300</sub> aggregates and control samples of pure  $C_{60}$ , PS homopolymer,  $C_{60}$ /PS blend and  $C_{60}$ /poly(methylmethacrylate) blend. Figure 9a shows the DSC scans of PS homopolymer (curve 1, the first and subsequent scans were identical), revealing a glass transition ( $T_g$ ) at 373 K which is in accord with literature values. The repeated DSC scans of  $C_{60}$  were identical (curve 2) to that shown in Figure 9a. The observed sharp endotherm at 259 K has previously been seen and assigned to the orientational phase transition of  $C_{60}$  from the simple cubic (sc) crystalline form which exists below 259 K to the face-centered cubic (fcc) crystalline form above 259 K.<sup>22</sup> We point out that the PPQ homopolymer does not exhibit any DSC transitions below 673 K. Also shown in Figure 9a is the first DSC scan of 3 wt %  $C_{60}$ /PPQ<sub>50</sub>PS<sub>300</sub> (curve 3) which reveals two second-order transitions with onset temperatures at 273 and 375 K, respectively. These two transition temperatures shifted slightly during subsequent scans, 269 and 374 K for the second run and 282 and 374 K for the third scan. It is noteworthy that the sc→fcc phase transition of pure  $C_{60}$  at 259 K was not observed in the DSC scan of  $C_{60}$ /PPQ<sub>50</sub>PS<sub>300</sub> aggregates. The aggregate transition at 374-375 K can be easily interpreted as the  $T_g$  of the PS block.<sup>38</sup> However, the aggregate second-order transition near 273 K is new and must be carefully assigned.

The DSC scan of a 1 wt %  $C_{60}$ /PS sample is shown in Figure 9b, revealing two second-order transitions at 274 and 373 K during the first run. The 373-K transition corresponds to the  $T_g$  of PS. The transition at 274 K shifted slightly to 270 K in subsequent scans. Similarly, the repeated DSC scans of  $C_{60}$  dispersed in poly(methylmethacrylate) (PMMA) (~1 wt %  $C_{60}$ )

gave a second-order transition at 270 K as well as the  $T_g$  transition of the polymer at 377 K<sup>38</sup> (not shown). The characteristic sc→fcc crystalline transition of pure  $C_{60}$  was not observed in either of the DSC scans of this fullerene in an amorphous polymer matrix (PS or PMMA). These results suggest that the new second-order transition at 270 K in the DSC scan of  $C_{60}$ /PPQ<sub>50</sub>PS<sub>300</sub> aggregates is characteristic of isolated or amorphous  $C_{60}$  dispersed in a polymer matrix. From these results we can also conclude that the  $C_{60}$  molecules encapsulated inside the block copolymer micelles are not crystalline and that at least some of them are close to and homogeneously dispersed in the PS block. This also supports the micellar mechanism of fullerene solubilization and encapsulation by PPQ-PS aggregates.

These studies of the morphology of self-organized fullerene/diblock copolymer aggregates in comparison with the empty micelles clearly reveal the profound effects of fullerene solubilization and encapsulation on the physical size and aggregation number. The observed increase in diameter of the fullerene/PPQ-PS spherical aggregates correlates well with amount of fullerene loading up to 70 mg/g and the underlying accommodation of more diblock chains per micellar aggregate. The previously discussed solubilization results together with the morphological observations and DSC results support our model structure of the rod-coil block copolymer micelles with encapsulated fullerene molecules shown in scheme 1. This structure assumes that the hollow cavity as well as the inner PS shell are partially filled with fullerene molecules whereas the rigid-rod PPQ outer shell is free of fullerenes.

**3. Effect of Encapsulated Fullerenes on Block Copolymer Assemblies.** We have exploited the intrinsic electroactive and photoactive properties of PPQ-PS block copolymers<sup>34, 35</sup> to probe molecular packing and the effects of encapsulated solubilizes on the molecular packing of the block copolymer assemblies. In particular, we focus on the molecular packing of

the conjugated rigid-rod PPQ block whose relative fluorescence quantum yield is orders of magnitude larger than those of the fullerenes ( $C_{60}$ ,  $C_{70}$ ). It is also noteworthy that the emission bands of the fullerenes are in the near infrared region, which is far away from where PPQ-PS aggregates emit, so that there is no possible interference from their fluorescence bands. As a reference chromophore, we investigated the photoluminescence emission (PL) and excitation (PLE) spectra of the isolated  $PPQ_{50}PS_{300}$  chain in the form of a dilute blend film [0.1 wt %  $PPQ_{50}PS_{300}$  in poly(ethylene oxide) (PEO)]. The PL spectrum of such an isolated  $PPQ_{50}PS_{300}$  chain had a peak at 466 nm (when excited at 380 nm) and a PLE spectrum with an absorption maximum at 390 nm when monitoring emission at 460 nm (not shown).

Figure 10a shows the PL and PLE spectra of a film of spherical  $PPQ_{50}PS_{300}$  aggregates without any fullerene. These spherical aggregate spectra are very similar to those of the isolated  $PPQ_{50}PS_{300}$  single chain except that they are slightly blue shifted. The aggregate PL spectrum has a peak at 454 nm whereas the PLE spectrum has a peak at 388 nm. Incorporation of fullerene molecules in  $PPQ_{50}PS_{300}$  aggregates results in dramatic changes in the aggregate photophysical properties as exemplified by Figure 10b which shows the PL and PLE spectra of a film of 1 wt %  $C_{60}/PPQ_{50}PS_{300}$ . Two emission bands at ~430 and ~600 nm are observed in the PL spectrum. The 430-nm emission band is blue-shifted compared to that of spherical  $PPQ_{50}PS_{300}$  aggregate without any  $C_{60}$  since the excitation spectra are similar whereas the 600-nm band is new. The PLE spectrum monitored at 480 nm gives an absorption band centered at 388 nm, slightly narrower (full width at half maximum of 62 versus 72 nm) than the spectrum of the empty  $PPQ_{50}PS_{300}$  aggregates. However, the PLE spectrum monitored at 600 nm shows entirely new absorption characteristics with peaks at 426 and 480 nm. These results suggest that the 430-nm and 600-nm emission bands come from different emitting species. Direct excitation

of the fullerene-PPQ<sub>50</sub>PS<sub>300</sub> aggregate at 480 nm gives an emission band that is the same as the 600-nm PL band. Figure 10c shows the PL and PLE spectra of aggregates of 5 wt % C<sub>60</sub>/PPQ<sub>50</sub>PS<sub>300</sub>. Only one emission band at 600 nm is observed regardless of the excitation wavelength. The corresponding PLE spectrum monitored at 600 nm showed absorption peaks at 429 and 506 nm. In fact, similar investigations of other compositions of encapsulated C<sub>60</sub> in PPQ<sub>50</sub>PS<sub>300</sub> between 0.1 and 5 wt % of C<sub>60</sub> showed a progressive evolution of the photophysical properties with fullerene loading.

We propose that these spectral features of the absorption and emission properties of fullerene/PPQ-PS assemblies can best be understood within the framework of H- and J-aggregation<sup>39-45</sup> of the rodlike PPQ blocks. The 454-nm emission band with corresponding 388-nm absorption band of the hollow PPQ<sub>50</sub>PS<sub>300</sub> micelles are blue-shifted from those of the isolated PPQ-PS chromophore, suggesting the occurrence of H-aggregation of the fluorescent PPQ blocks. The further blue shift and narrowing of the 430-nm emission band at 1 wt% C<sub>60</sub> loading suggest that the H-aggregates of PPQ blocks are modified compared to the empty PPQ<sub>50</sub>-PS<sub>300</sub> assemblies. The significantly red-shifted absorption (PLE) and emission bands at 506 and 600 nm, respectively, in the 5 wt % C<sub>60</sub>/PPQ<sub>50</sub>PS<sub>300</sub> assemblies compared to the isolated PPQ-PS chromophore are characteristic of J-aggregation of the conjugated PPQ blocks. The progressive evolution of the PLE and PL spectra with increasing amount of fullerene molecules incorporated into the PPQ-PS assemblies can thus be understood as a consequence of the progressive transformation of the H-aggregates of PPQ blocks in the original empty hollow micelles into all J-aggregates at 5 wt % C<sub>60</sub> loading which corresponds to 3.1 C<sub>60</sub> molecules per PPQ<sub>50</sub>PS<sub>300</sub> copolymer chain. Such a fullerene solubilization and encapsulation induced transformation of

PPQ-PS rod-coil diblock copolymer chains in H-aggregates to J-aggregates is illustrated in scheme 2.

These results further confirm the profound effects of fullerene solubilization and encapsulation on the aggregation behavior of the rod-coil diblock copolymers and their micellar assemblies. The strong interaction of the fullerenes with PS blocks and consequently on the molecular packing of the PPQ blocks also support the micellar nature of the hollow spherical aggregates of PPQ-PS rod-coil block copolymers. Although the possible contribution of some vesicle-like trapping to the fullerene solubilization in PPQ-PS assemblies cannot be completely ruled out, all the present results support micellar solubilization as the dominant mechanism. For example, trapped molecules in bilayer vesicles do not usually influence the molecular packing of the hollow spheres.<sup>37</sup> We also note that the J-aggregation of conjugated PPQ blocks in the spherical fullerene/PPQ-PS block copolymer assemblies confirm that the fullerene molecules are excluded from the outer shell PPQ blocks (schemes 1 and 2).

The observed J-aggregation of these self-organized fullerene-block copolymer micelles imply that they are highly ordered.<sup>39-45</sup> This is in accord with the previously discussed polarized optical microscopy observations (Figures 4-6). Together, these results provide unusually detailed knowledge of molecular packing and of the effects of solubilizates on the molecular packing of block copolymer micelles, demonstrating the potential of optical and photoelectronic techniques for characterizing micellar aggregates containing electroactive and photoactive blocks. The fullerene-block copolymer assemblies *per se* are also of potential broad interest as advanced mesoscopic materials with possible *cooperative* electronic and optical properties similar to molecular aggregates of dyes<sup>39-45</sup> and composite properties that combine those of the fullerenes and conjugated polymers.<sup>22-28</sup> Development of methods to order or crystallize or dope

the encapsulated fullerenes inside the block copolymer micelles could open up many other possible applications of these supramolecular materials.

## Conclusions

Ultralarge hollow micelles ( $>1\ \mu\text{m}$ ) formed by rod-coil diblock copolymers, poly(phenylquinoline)-*block*-polystyrene (PPQ-PS), in *protic* organic solvents have been explored for the solubilization and encapsulation of fullerenes  $\text{C}_{60}$  and  $\text{C}_{70}$ . High solubilization capacity and large enhancement of fullerene solubility have been demonstrated. Micellization and solubilization phenomena in surfactants and coil-coil block copolymers have heretofore been observed on the scale of 2-10 nm and 20 –100 nm, respectively, which correspond to the self-organized structures formed by the relevant amphiphiles.<sup>1-20</sup> The present results thus provide the first evidence of micellization and micellar solubilization phenomena at the 1-30  $\mu\text{m}$  size scale. Although theoretical elucidation of these phenomena at such a large scale is currently lacking, many practical advantages can be envisioned; for example, increase in capacity of a chemical extraction process and ability to solubilize or encapsulate large molecules and nanoparticles such as dendrimers and derivatized semiconductor nanoparticles.

The solubilization and encapsulation of  $10^7$  to  $10^{10}$  fullerene molecules per PPQ-PS block copolymer micelle results in a large increase of aggregation number to over  $10^9$  and of physical size to 30  $\mu\text{m}$ . Introduction of fullerene  $\text{C}_{60}$  or  $\text{C}_{70}$  into a solution of PPQ-PS block copolymer alters the micellization and self-assembly process from formation of many different aggregates to the selective formation of ultralarge hollow spheres that sequester the fullerene molecules. Photoluminescence emission and excitation spectroscopy of the self-organized fullerene-block copolymer assemblies has provided evidence of fullerene-induced J-aggregation of the conjugated PPQ blocks and in the process clearly reveals the effects of solubilizate on molecular

packing of block copolymer micelles. Finally, we believe that the fullerene-block copolymer assemblies are interesting supramolecular materials with potential composite or cooperative properties.

### **Acknowledgements**

This research was supported by the Office of Naval Research and in part by the National Science Foundation (CTS-9311741 and CHE-9120001) and an Elon Huntington Hooker Fellowship to X. L. C.

## REFERENCES

- (1) *Solvents and Self-Organization of Polymers*, Webber, S. E.; Munk, P.; Tuzar, Z., Eds; Kluwer Academic Publishers: Dordrecht, The Netherlands, 1996.
- (2) Webber, S. E. *J. Phys. Chem. B* **1998**, *102*, 2618.
- (3) Tuzar, Z.; Kratochvil, P. In *Surface and Colloid Science*, vol. 15, Matijević, E., Ed.; Plenum Press: New York, 1993; pp. 1-83.
- (4) Halperin, A.; Tirrell, M.; Lodge, T. P. *Adv. Polym. Sci.* **1992**, *100*, 31.
- (5) Förster, S.; Antonietti, M. *Adv. Mater.* **1998**, *10*, 195.
- (6) (a) Zhang, L.; Eisenberg, A. *J. Am. Chem. Soc.* **1996**, *118*, 3168. (b) Zhang, L.; Eisenberg, A. *Science* **1995**, *268*, 1728.
- (7) (a) Nagarajan, R.; Ganesh, K. *Macromolecules* **1989**, *22*, 4312. (b) Nagarajan, R.; Ganesh, K. *J. Chem. Phys.* **1989**, *90*, 5843.
- (8) (a) Hurter, P. N.; Scheutjens, J. M. H. M.; Hatton, T. A. *Macromolecules* **1993**, *26*, 5030. (b) Hurter, P. N.; Scheutjens, J. M. H. M.; Hatton, T. A. *Macromolecules* **1993**, *26*, 5592.
- (9) Linse, P. *Macromolecules* **1994**, *27*, 2685.
- (10) Cogan, K. A.; Leermakers, F. A. M.; Gast, A. P. *Langmuir* **1992**, *8*, 429.
- (11) Xing, L.; Mattice, W. L. *Macromolecules* **1997**, *30*, 1711.
- (12) Nagarajan, R.; Barry, M.; Ruckenstein, E. *Langmuir* **1986**, *2*, 210.
- (13) Zhou, Z.; Chu, B. *J. Colloid Interface Sci.* **1988**, *126*, 171.
- (14) (a) Cogan, K. A.; Gast, A. P. *Macromolecules* **1990**, *23*, 745. (b) Cogan, K. A.; Capel, M.; Gast, A. P. *Macromolecules* **1991**, *24*, 6512.

- (15) (a) Alexandridis, P.; Holzwarth, J. F.; Hatton, T. A. *Macromolecules* **1994**, 27, 2414.  
(b) Alexandridis, P.; Nivaggioli, T.; Hatton, T. A. *Langmuir* **1995**, 11, 1468. (c) Hurter, P. N.; Hatton, T. A. *Langmuir* **1992**, 8, 1291.
- (16) Tian, M.; Arca, E.; Tuzar, Z.; Webber, S. E.; Munk, P. *J. Polym. Sci., Part B: Polym. Phys.* **1995**, 33, 1713.
- (17) Vagberg, L. J. M.; Cogan, K. A.; Gast, A. P. *Macromolecules* **1991**, 24, 1670.
- (18) Kiserow, D.; Prochazka, K.; Ramireddy, C.; Tuzar, Z.; Munk, P.; Webber, S. E. *Macromolecules* **1992**, 25, 461.
- (19) (a) Price, C.; Stubbersfield, R. B. *Eur. Polym. J.* **1987**, 23, 177; (b) Quintana, J. R.; Salazar, R. A.; Katime, I. *Macromolecules* **1994**, 27, 665; (c) Quintana, J. R.; Salazar, R. A.; Katime, I. *J. Phys. Chem.* **1995**, 99, 3723.
- (20) Wang, G.; Henselwood, F.; Liu, G. *Langmuir* **1998**, 14, 1554.
- (21) Jenekhe, S. A.; Chen, X. L. *Science* **1998**, 279, 1903.
- (22) Dresselhaus, M. S.; Dresselhaus, G.; Eklund, P. C. *Science of Fullerenes and Carbon Nanotubes*; Academic Press: San Diego, CA, 1996.
- (23) Hirsch, A. *The Chemistry of the Fullerenes*; Georg Thieme Verlag: Stuttgart, 1994.
- (24) *The Chemical Physics of Fullerenes 10 (and 5) Years Later*, Andreoni, W., Ed.; Kluwer Academic Publishers: Dordrecht, The Netherlands, 1996.
- (25) Hebard, A. F.; Rosseinsky, M. J.; Haddon, R. C.; Murphy, D. W.; Glarum, S. H.; Palstra, S. H.; Ramirez, T. T. M.; Kortan, A. R. *Nature* **1991**, 350, 600.
- (26) (a) Zakhidov, A. A.; Araki, H.; Tada, K.; Yakushi, K.; Yoshino, K. *Phys. Lett. A* **1995**, 205, 317. (b) Kajii, H.; Araki, H.; Zakhidov, A. A.; Yakushi, K.; Yoshino, K. *Synth. Met.* **1997**, 86, 2351.

- (27) (a) Sariciftci, N. S.; Smilowitz, L.; Heeger, A. J.; Wudl, F. *Science* **1992**, 258, 1474.  
(b) Sariciftci, N. S.; Braun, D.; Zhang, C.; Srdanov, V. I.; Heeger, A. J.; Stucky, G.; Wudl, F. *Appl. Phys. Lett.* **1993**, 62, 585.
- (28) (a) Wang, Y. *Nature* **1992**, 356, 585. (b) Wang, Y.; Suna, A. *J. Phys. Chem. B* **1997**, 101, 5627.
- (29) Ruoff, R. S.; Tse, D. S.; Malhotra, R.; Lorents, D. C. *J. Phys. Chem.* **1993** 97, 3379.
- (30) Sivaraman, N.; Dhamodaran, R.; Kaliappan, I.; Srinivasan, T. G.; Vasudeva Rao, P. R.; Mathews, C. K. *J. Org. Chem.* **1992** 57, 6077.
- (31) Evans, D. F.; Wennerström, H. *The Colloidal Domain: Where Physics, Chemistry, Biology, and Technology Meet*; Wiley-VCH: New York, 1994.
- (32) Chen, X. L.; Jenekhe, S. A. *J. Am. Chem. Soc.* To Be Submitted.
- (33) Sybert, P. D.; Beever, W. H.; Stille, J. K. *Macromolecules* **1981**, 14, 493.
- (34) (a) Agrawal, A. K.; Jenekhe, S. A. *Macromolecules* **1993**, 26, 895. (b) Agrawal, A. K.; Jenekhe, S. A. *Chem. Mater.* **1996**, 8, 579.
- (35) (a) Agrawal, A. K.; Jenekhe, S. A.; Vanherzeele, H.; Meth, J. S.; *J. Phys. Chem.* **1992**, 96, 2837. (b) Jenekhe, S. A.; Zhang, X.; Chen, X. L.; Choong, V.-E.; Gao, Y.; Hsieh, B. R. *Chem. Mater.* **1997**, 9, 409.
- (36) (a) Osaheni, J. A.; Jenekhe, S. A. *J. Am. Chem. Soc.* **1995**, 117, 7389. (b) Jenekhe, S. A.; Osaheni, J. A. *Science* **1994**, 265, 765.
- (37) *Vesicles*, Rosoff, M., Ed.; Marcel Dekker: New York, 1996.
- (38) *Polymer Handbook*, 3rd ed., Brandrup, J.; Immergut, E. H., Ed.; Wiley: New York, 1989; Chapt. V, pp. 77-86.
- (39) Kasha, M. *Radiation Research* **1963**, 20, 55.

- (40) Czikkely, V.; Försterling, H. D.; Kuhn, H. *Chem. Phys.* **1970**, *6*, 11.
- (41) Fidler, H.; Wiersma, D. A. *Phys. Stat. Sol. B* **1995**, *188*, 285.
- (42) Hochstrasser, R. M.; Kasha, M. *Photochem. Photobiology* **1964**, *3*, 317.
- (43) Chen, H.; Farahat, M. S.; Law, K.-Y.; Whitten, D. G. *J. Am. Chem. Soc.* **1996**, *118*, 2584.
- (44) Grätzel, M.; Nüesch, F. *Chem. Phys.* **1995**, *193*, 1.
- (45) Spano, F. C.; Mukamel, S. *Phys. Rev. A* **1989**, *40*, 5783.

## FIGURE CAPTIONS

Figure 1. Optical absorption spectra of solutions of (a) pure PPQ<sub>50</sub>PS<sub>300</sub> (1:1 TFA:DCM, 0.05 wt %), (b) 5 wt % C<sub>60</sub>/ PPQ<sub>50</sub>PS<sub>300</sub> (1:1 TFA:DCM, 0.05 wt %), and (c) C<sub>60</sub> in CS<sub>2</sub> (0.05 wt %). Inset is the magnified spectrum of the 5 wt % C<sub>60</sub>/ PPQ<sub>50</sub>PS<sub>300</sub> in the region of 450-700 nm.

Figure 2. Optical absorption spectra of solutions of 5 wt % C<sub>70</sub>/ PPQ<sub>50</sub>PS<sub>300</sub> and 5 wt % C<sub>70</sub>/ PPQ<sub>10</sub>PS<sub>300</sub> (1:1 TFA:DCM, 0.05 wt %). Also shown for comparison are the spectra of C<sub>70</sub> in CS<sub>2</sub> (0.05 wt %) and pure PPQ<sub>50</sub>PS<sub>300</sub> (1:1 TFA:DCM, 0.05 wt %).

Figure 3. Normalized absorbance of fullerene-PPQ-PS solutions as a function of fullerene loading: (a) C<sub>60</sub>-PPQ-PS system and (b) C<sub>70</sub>-PPQ-PS system. The solvent is TFA/DCM (1/1, v/v).

Figure 4. Fluorescence (a, b) and polarized optical (c) micrographs of aggregates of PPQ<sub>50</sub>PS<sub>300</sub> containing 0.1 wt % solubilized C<sub>70</sub> and (d) fluorescence optical micrograph of 0.1 wt% C<sub>60</sub> in PPQ<sub>50</sub>PS<sub>300</sub>.

Figure 5. Fluorescence (a, b) and polarized optical (c) micrographs of aggregates of PPQ<sub>50</sub>-PS<sub>300</sub> containing 1 wt % solubilized C<sub>60</sub> prepared from 4:1 TFA:toluene.

Figure 6. Fluorescence (a, c) bright field (b) and polarized optical (d) micrographs of aggregates of PPQ<sub>50</sub>-PS<sub>300</sub> containing 6 wt % solubilized C<sub>60</sub> prepared from 1:1 TFA:DCM.

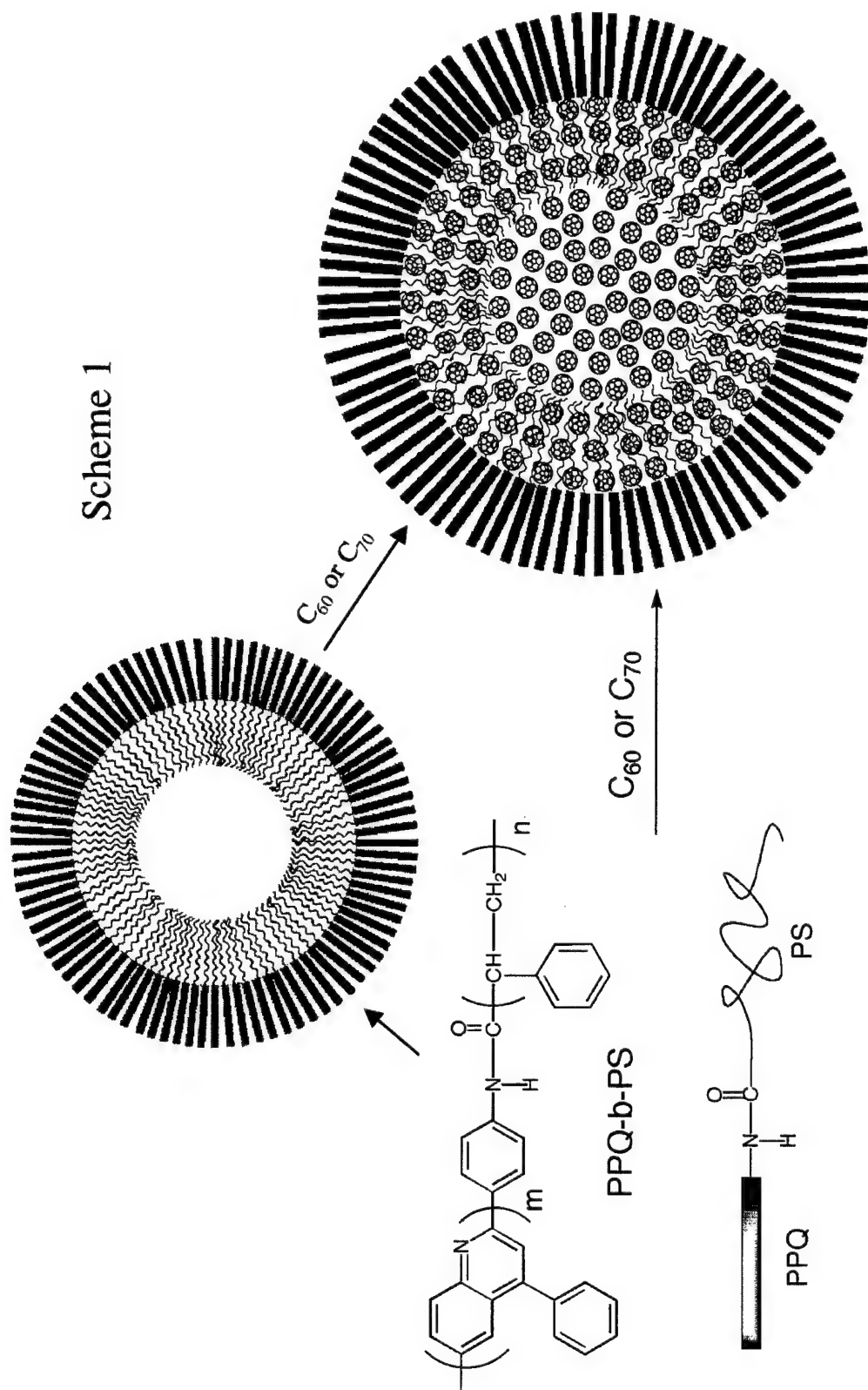
Figure 7. Bright field optical micrographs of films of PPQ<sub>50</sub>PS<sub>300</sub> aggregates dried from solutions containing 8 wt % (a) and 10 wt % (b) C<sub>60</sub>.

Figure 8. Average diameters of spherical fullerene/PPQ-PS aggregates as a function of fullerene loading and block copolymer composition. The line is only a guide to eyes.

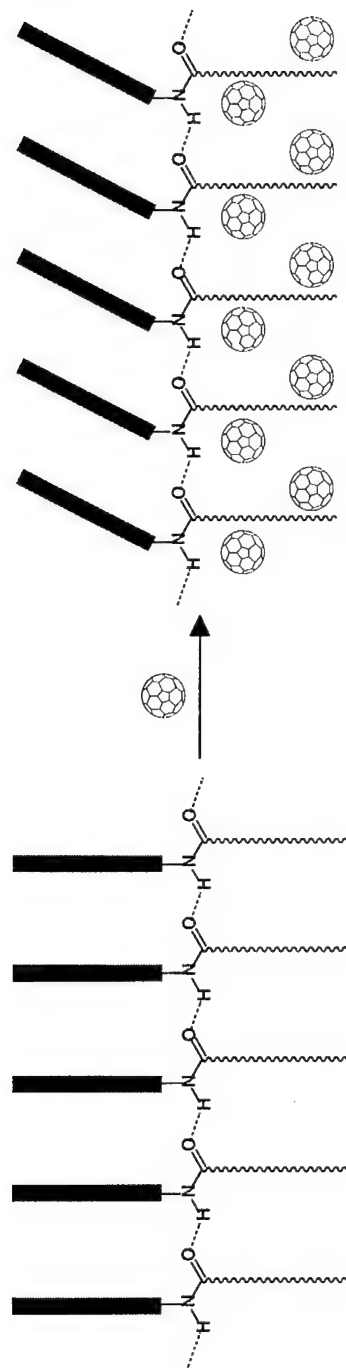
Figure 9. (a) DSC scans of PS homopolymer (1), pure  $C_{60}$  (2), and 3 wt %  $C_{60}/PPQ_{50}PS_{300}$  aggregates. (b) DSC scans of 1 wt %  $C_{60}$  dispersed in PS homopolymer. Inset is the scan magnified in the region 250K to 290K.

Figure 10. PL and PLE spectra of spherical  $PPQ_{50}PS_{300}$  aggregates containing no  $C_{60}$  (a), 1 wt%  $C_{60}$  (b) and 5 wt%  $C_{60}$  (c). The excitation wavelength for the PL spectra were 380 nm (a), 360 nm (curve 1) and 475 nm (curve 2) (b), and 475 nm (c). The emission wavelengths monitored for the PLE spectra were 480 nm (a), 480 nm (curve 3) and 600 (curve 4) (b), and 600 nm (c).

Scheme 1



Scheme 2



(a)

(b)

Figure 1

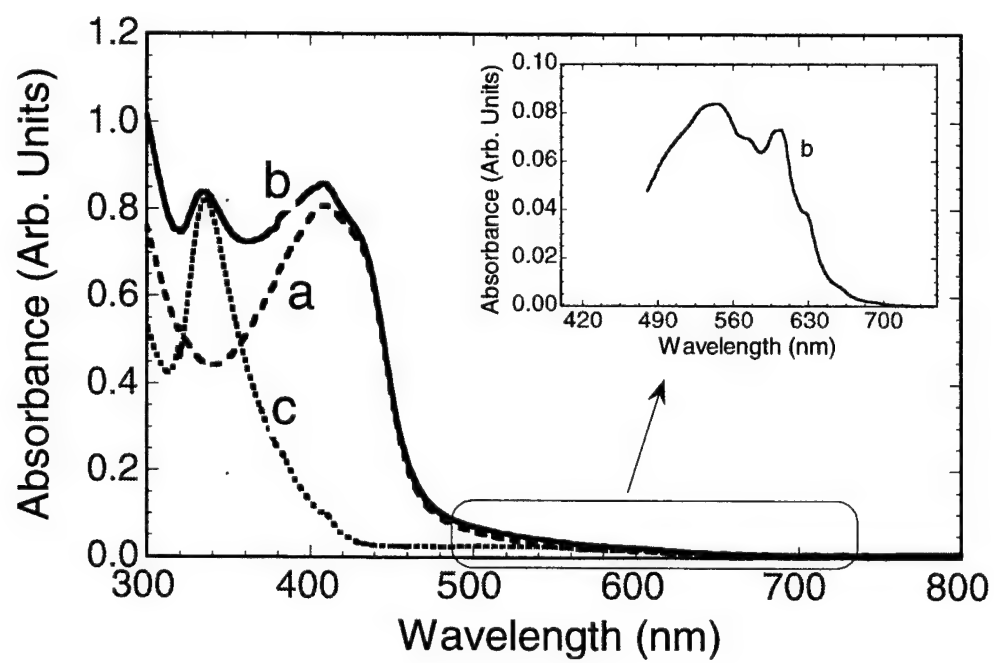


Figure 2

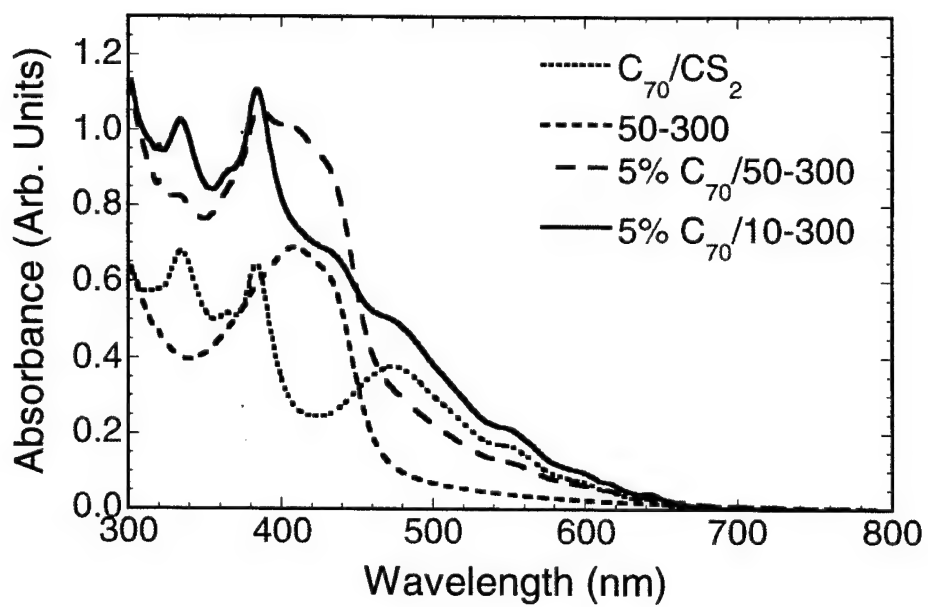


Figure 3

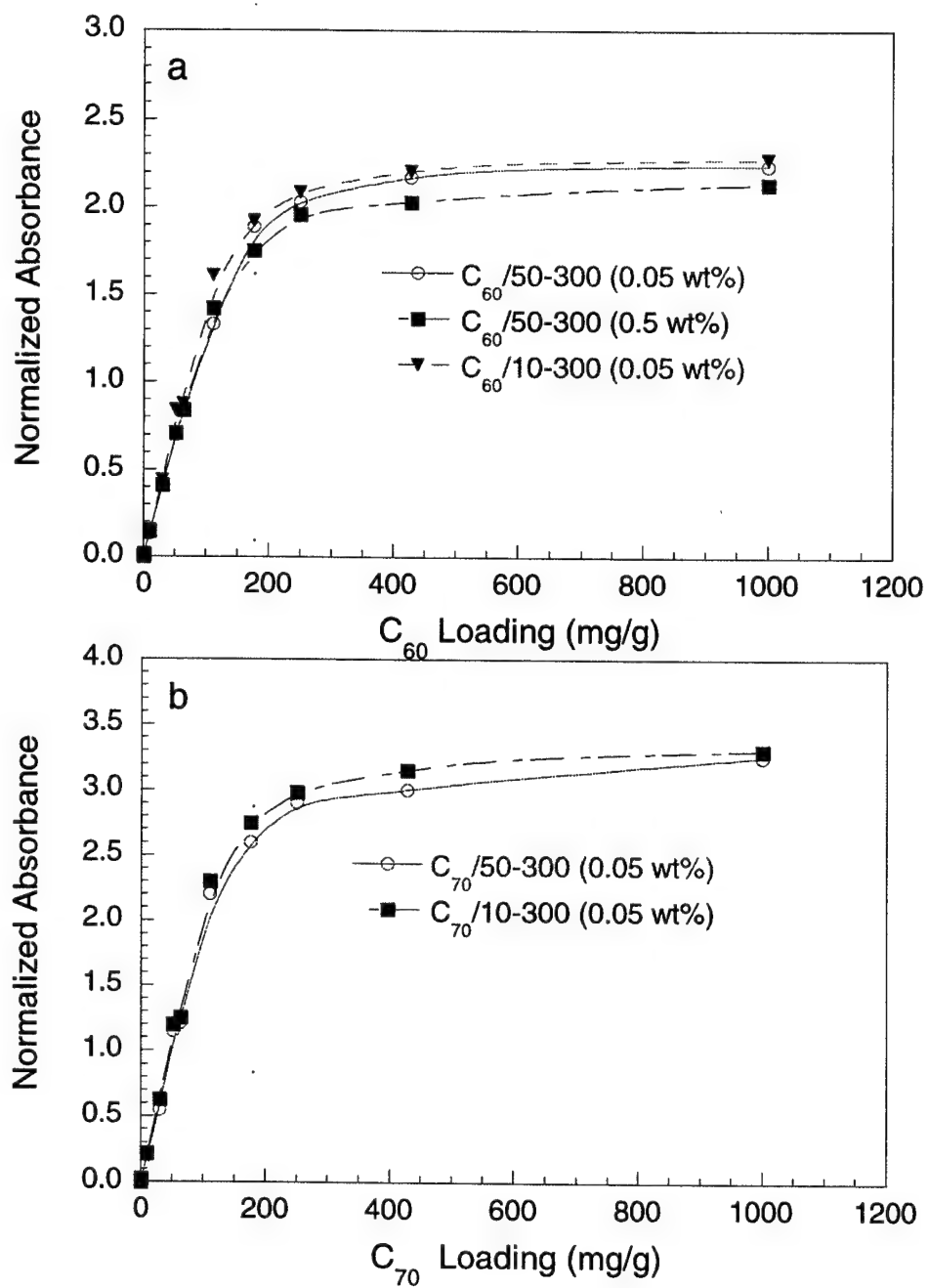


Figure 4

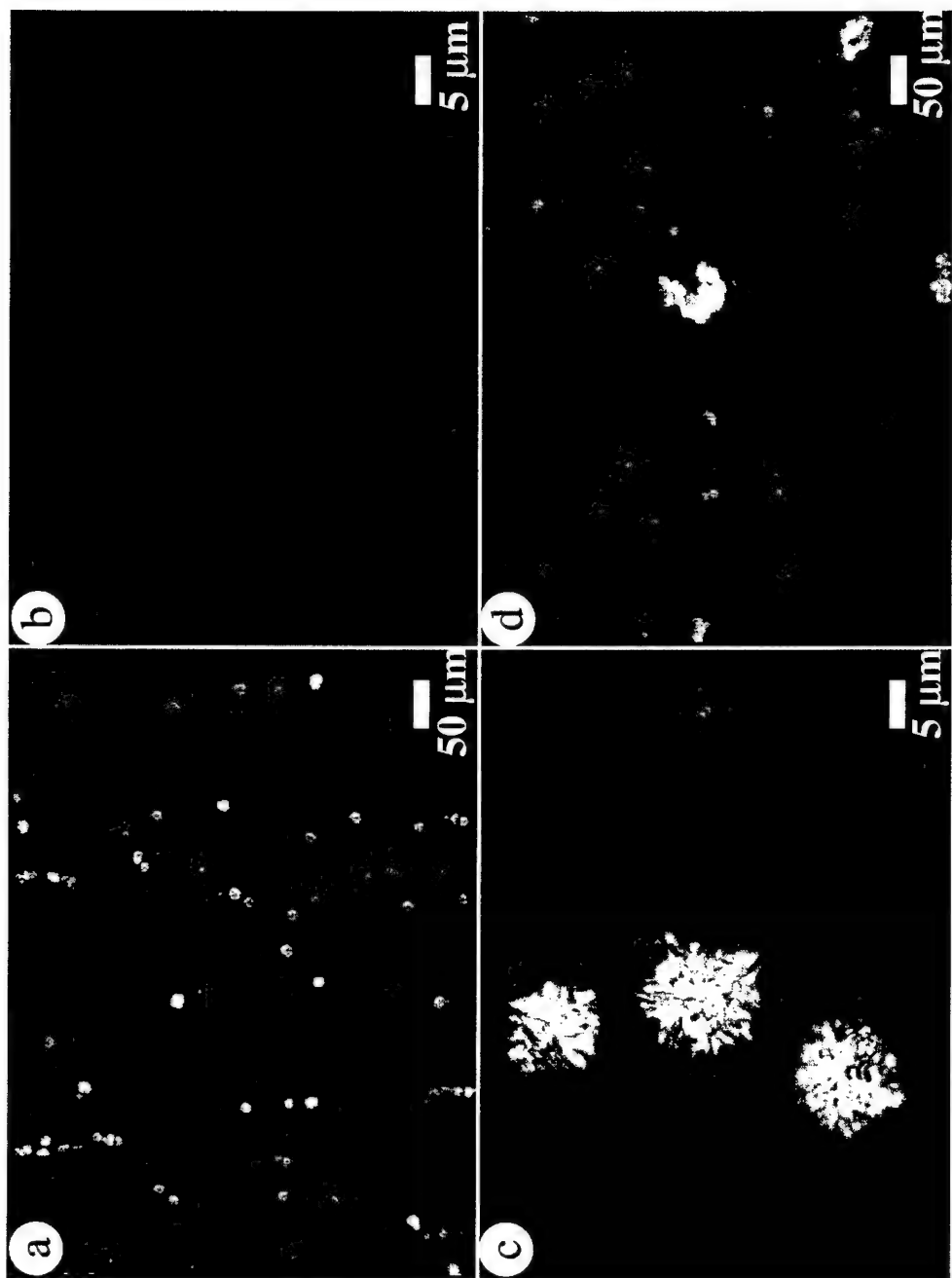


Figure 5

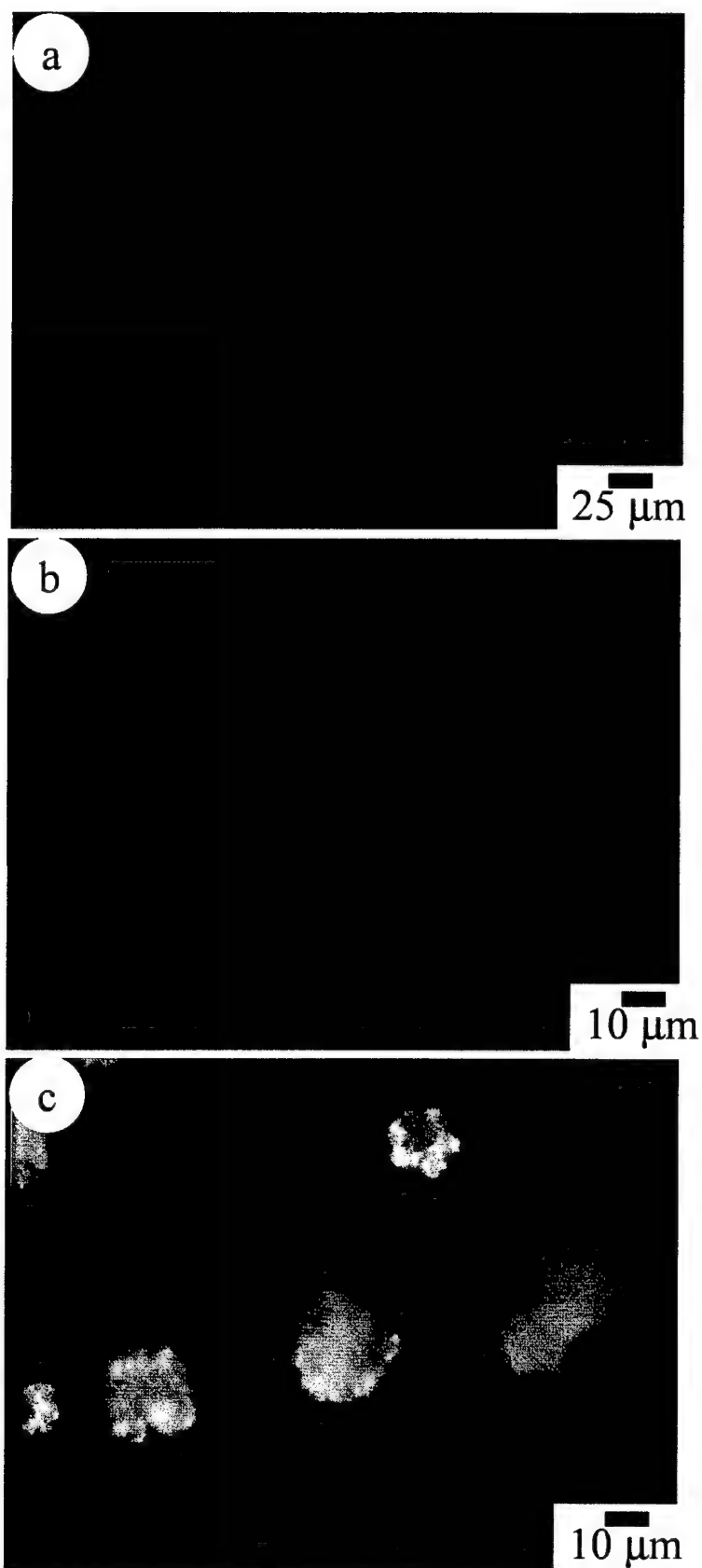


Figure 6

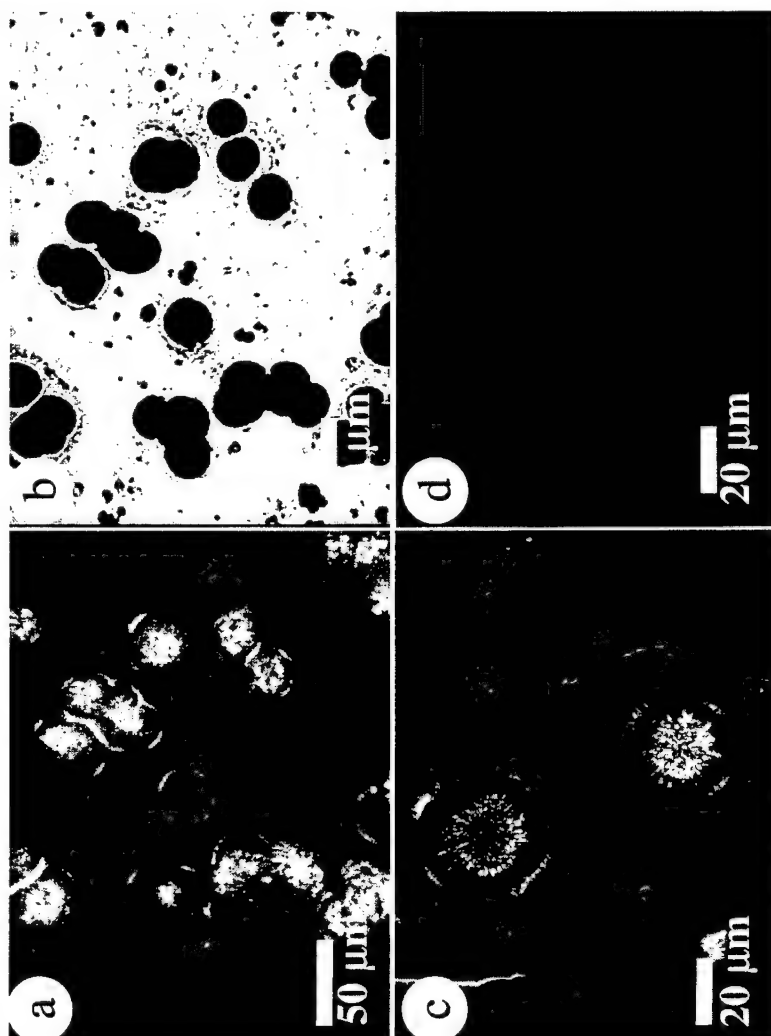


Figure 7

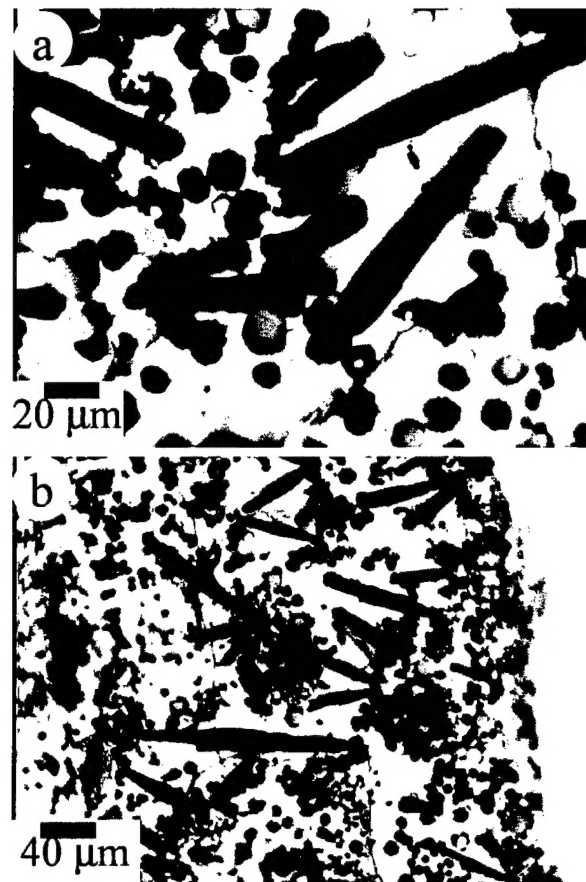


Figure 8

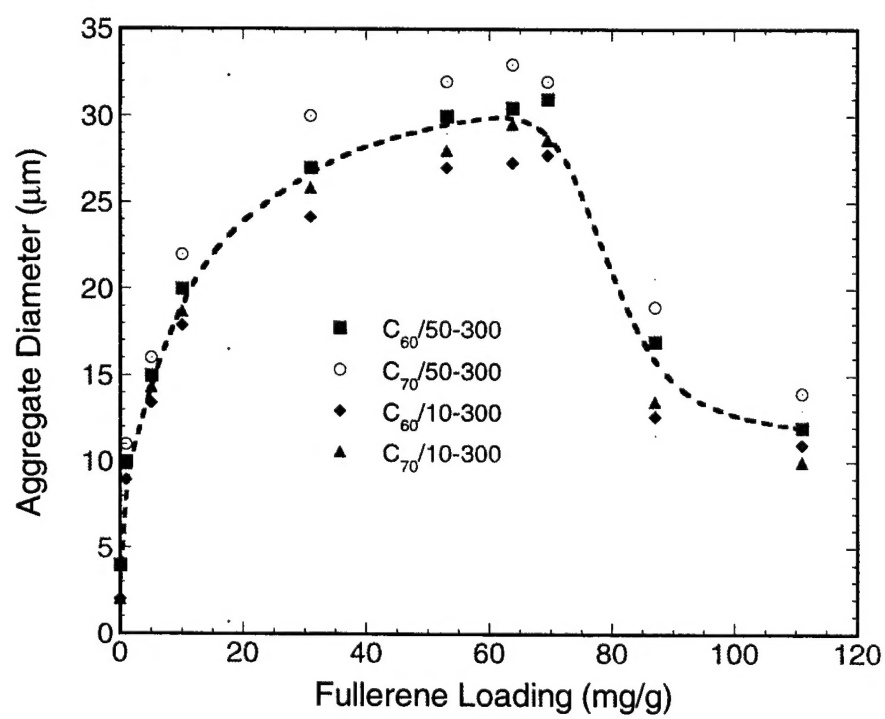


Figure 9

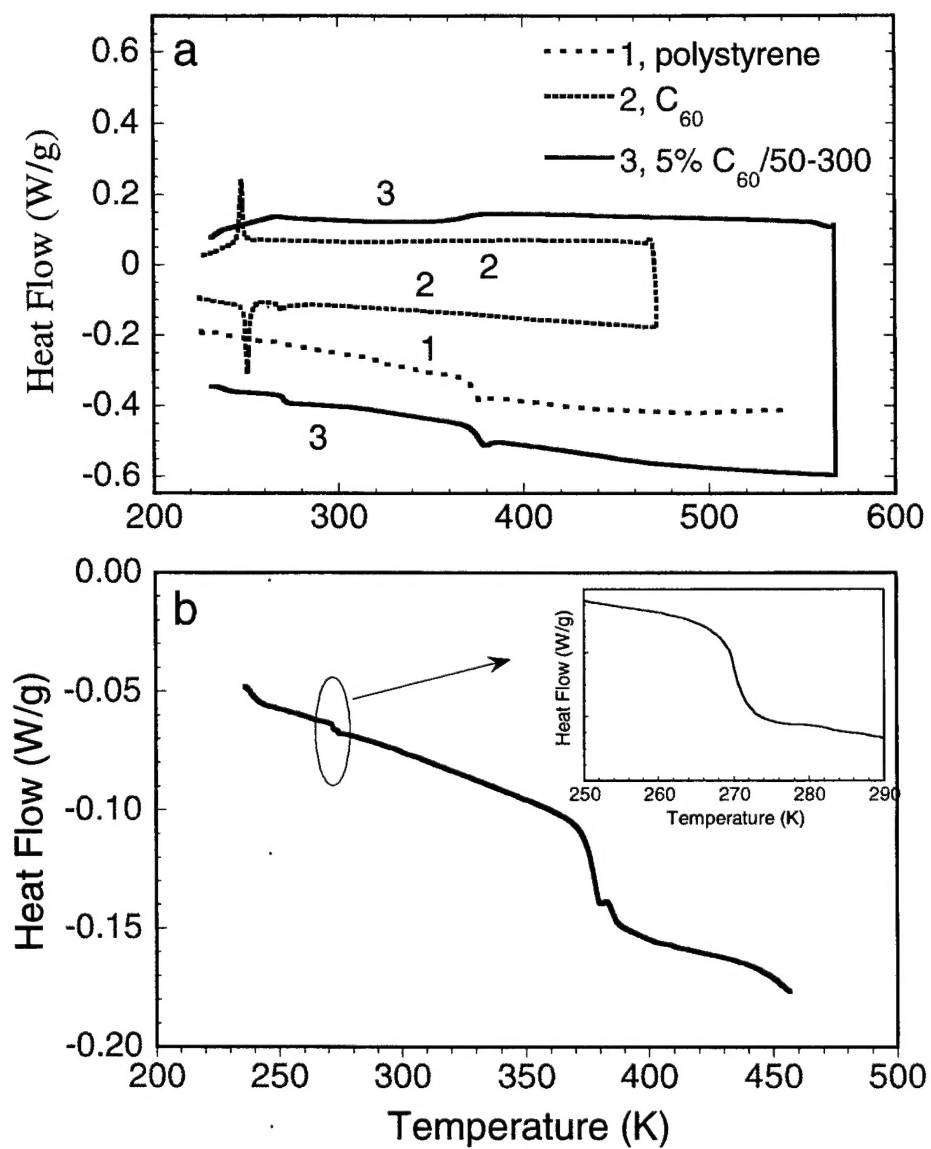


Figure 10

